New Data on the Structure of Uranium Monocarbide

N. Vigier,[†] C. Den Auwer,*[,†] C. Fillaux,[†] A. Maslennikov,[‡] H. Noël,[§] J. Roques,[||] D. K. Shuh,[⊥] E. Simoni,[||] T. Tyliszczak,[⊥] and P. Moisy[†]

CEA Marcoule, DEN/DRCP/SCPS, 30207 Bagnols sur Cèze, France, Institute of Physical Chemistry and Electrochemistry, Russian Academy of Sciences, 31 Leninsky Prospect, 119991 Moscow, Russian Federation, Laboratoire de Chimie du Solide et Matériaux, UMR CNRS 6226, Université de Rennes 1, Avenue du Général Leclerc, 35042 Rennes, France, IPN Orsay, Université Paris XI Orsay, 91405 Orsay, France, and Lawrence Berkeley National Laboratory, 1 Cyclotron Road, Berkeley, California 94720

Received January 18, 2008. Revised Manuscript Received February 28, 2008

Uranium monocarbide (UC) or ternary alloys are considered to be possible candidates for future nuclear fuels. Although the crystallographic and electronic structure of UC has been addressed in past investigations, discrepancies in the literature data have fostered a new investigation of the UC phase. We report here a reinvestigation of the UC phase by complementary X-ray spectroscopy and quantum chemical calculations. A combination of X-ray powder diffraction and extended X-ray absorption fine structure analysis at the uranium L_{III} edge led to the crystallographic determination of the UC phase of the NaCl type. For electronic structure investigation, a combination of uranium X-ray absorption near-edge spectroscopy at the L_{III} edge and at the $N_{IV,V}$ edges with quantum chemical calculations allowed us to define the evolution of the metal charge in comparison with metallic uranium on the one hand and uranium dioxide on the other hand.

Introduction

Uranium monocarbide (UC) or ternary (U,Pu)C is considered to be one of the possible candidates for use as a kernel material in TRISO fuel of IVth generation reactors. The possibility to incinerate minor actinides and some long-lived fission products (^{99}Tc, ^{129}I, and ^{79}Se) during the fuel burn-up is considered to be one of the advantages of high-temperature gas-cooled reactors (HTGR).[1,2] The complex design of the HTGR fuel assemblies and low fissile material content (about 4.0% instead of 70% for light water reactors (LWR)) in the graphite compacts would require a significant increase in the actinide recovery at the head end of the reprocessing.[3] The development of aqueous techniques for UC based fuel reprocessing faces the problem of the removal of organic compounds from the dissolver solution. These compounds are formed during UC oxidation in aqueous solutions and exhibit adverse effects on the U(VI) and Pu(IV) extraction.[4] Therefore, the data on the nature of chemical bonding in UC seem to be essential for the understanding of the mechanism of UC oxidation in aqueous solutions and consequently for the development of the effective dissolution technique of UC based TRISO fuel. This application followed the previous report on the study of UC electrochemistry and UC oxidation with nitrous acid in solutions of HNO_3 and $HClO_4$.[5]

The crystal structure of UC was the subject of former reports in 1948.[6–8] We report herein a set of new data from powder X-ray diffraction (XRD) and X-ray absorption spectroscopy (XAS) in both XANES (X-ray absorption near-edge spectroscopy) and EXAFS (extended X-ray absorption fine structure) regimes. Moreover, to our knowledge, very few theoretical studies of the fully relaxed structures of UC have been carried out up to now. In this way, several calculations were performed in the DFT-generalized gradient approximation (GGA) formalism to obtain both structural parameters and electronic properties of the UC bulk system, as compared to α-U. The combination of XRD, EXAFS data, and DFT calculations demonstrated unambiguously that UC has a NaCl structural type. Additional measurements at the uranium absorption edge (both L_{III} and $N_{IV,V}$ edges) and the calculated electronic structure suggest that the electronic character of uranium lies in between metallic uranium and uranium dioxide.

Experimental Procedures

Synthesis. Samples of uranium monocarbide with an approximate weight of 1 g were prepared by melting in an arc furnace

* Corresponding author. E-mail: christophe.denauwer@cea.fr.
[†] CEA Marcoule.
[‡] Russian Academy of Sciences.
[§] Université de Rennes 1.
[||] Université Paris XI Orsay.
[⊥] Lawrence Berkeley National Laboratory.

(1) Kuijper, J. C.; Raepsaet, X.; de Haas, J. B. M.; von Lensa, W.; Ohlig, U.; Ruetten, H.-J.; Brockmann, H.; Damian, F.; Dolci, F.; Bernnat, W.; Oppe, J.; Kloosterman, J. L.; Cerullo, N.; Lomonaco, G.; Negrini, A.; Magill, J.; Seiler, R. *Nucl. Eng. Des.* **2006**, *236*, 615.
(2) Bakster, A.; Rodriguez, C. *Progr. Nucl. Energy* **2001**, *38*, 81.
(3) Masson, M.; Grandjean, S.; Lacquement, J.; Bourg, S.; Delauzun, J.-M.; Lacombe, J. *Nucl. Eng. Des.* **2006**, *236*, 516.
(4) Choppin, G. R.; Bokelund, H.; Caceci, M. S.; Valkiers, S. *Radiochim. Acta* **1983**, *34*, 151.
(5) Maslennikov, A.; Fourest, B.; Sladkov, V.; Moisy, P. *J. Alloys Compd.* **2007**, *445–445*, 550.
(6) Litz, L. M.; Garrett, A. B.; Croxton, F. C. *J. Am. Chem. Soc.* **1948**, *70*, 1718.
(7) Rundle, R. E.; Baenziger, N. C.; Wilson, A. S.; McDonald, R. A. *J. Am. Chem. Soc.* **1948**, *70*, 99.
(8) Austin, A. E. *Acta Crystallogr.* **1959**, *12*, 159.

10.1021/cm8001783 CCC: $40.75
Published on Web 04/02/2008

stoichiometric amounts of depleted uranium metal and carbon graphite (nuclear grade). The U platelets were surface cleaned in diluted nitric acid prior to use, and a piece of the Ti−Zr alloy was first melted to remove all traces of oxygen from the argon atmosphere in the arc furnace. As UC melts congruently, annealing is not necessary to obtain a pure phase.

Preparation of EXAFS UC and U Metal Samples. The UC ingots were crushed and ground in an agate mortar under atmosphere to give a UC powder with a particle size of 50–100 μm. The U metal foil sample (10 μm) was etched in a solution of 4.0 M HNO_3 and 0.01 M HF (30 s at room temperature) to remove the surface oxide, rinsed with water and acetone, and dried in Ar. It was then sealed with Kapton tape. UO_2 was prepared by oxalic conversion via precipitation of U(IV) under controlled conditions (slight excess of $H_2C_2O_4$ in acidic media). The resulting crystallized powder was filtered off, washed and dried at room temperature, and thermally treated up to 900 °C for 10 hours, under an argon/H_2 (95:5 vol %) flow.

X-ray Absorption Spectroscopy. UC an U metal uranium L_{III} edge spectra were recorded at the Rossendorf beamline (ROBL)[9] at ESRF (6.0 GeV at 200 mA) in fluorescence mode, at room temperature, with a Si(111) water-cooled monochromator in a channel cut mode. Two Pt coated mirrors were used for harmonic rejection. The UO_2 spectrum was recorded at the former LURE facility on a D44 beamline equipped with a Ge(400) double crystal monochromator, in transmission mode. In all cases, energy calibration was carried out with Y foil (17052.0 eV at the absorption maximum). Data treatment (AUTOBK normalization) was performed with the Athena[10] code. XANES normalization was performed up to $k = 10$ Å^{-1}. Data fitting was carried out with the Artemis code in R space between 1.6 and 5.1 Å after Fourier transformation (Kaiser window between 2.0 and 14.7 Å^{-1}). Phases and amplitudes were calculated by the Feff82[11] code from a model cluster of a NaCl type with a lattice parameter of 4.956 Å where the uranium atoms were positioned in a face centered cubic (fcc) lattice. In the fit, a total of two single and five multiple scattering paths were included: single paths U−C and U−U from the first neighbors, triangular triple paths from the C and U first neighbors, and forward scattering (linear) triple and quadruple paths from the C and U first neighbors. All the paths were structurally linked to the U−C distance that is equal to half the lattice distance. Only the energy threshold shift variable e_0, one global amplitude factor S_0^2, and one Debye–Waller factor for multiple scattering paths were used. The number of neighbors and/or path degeneracy was fixed according to the NaCl type of the structure. Data were not corrected from self-absorption; this correction is de facto included in the fitted global amplitude factor S_0^2 (this explains the low value of S_0^2 in the fit as compared to the typical values between 0.9 and 1.0).

The uranium $N_{IV,V}$ edge spectrum was recorded with a scanning transmission X-ray microscope end station at the Advanced Light Source Molecular Environmental Science (ALS-MES) beamline 11.0.2 at the Lawrence Berkeley National Laboratory (LBNL). The ALS-MES beamline is particularly convenient for performing soft X-ray experiments with radioactive materials.[12]

Powder XRD. X-ray powder diffraction was carried out with a CPS120 INEL diffractometer in the Debye–Scherrer geometry. The X-ray source was a Cu Kα anticathode equipped with a germanium monochromator. Twenty milligrams of UC powder was ground with 10 mg of an internal reference (Au_NIST) and placed on a plate in the goniometer. Data refinement was carried out with the FullProf[13] code from the NaCl ($Fm3m$) and ZnS ($F\bar{4}3m$) structural types.

Computational Details. All DFT periodic calculations were performed using the Vienna ab initio simulation package, VASP 4.6.[14–17] The electronic density was optimized with the GGA as defined by Perdew et al.,[18,19] which has proven to be better for f-electron metals than the more commonly used LDA.[20] All atoms were described with pseudopotentials developed on plane wave basis sets generated with the projector augmented wave (PAW) method[21] and parametrized for GGA. Carbon atoms were composed of four valence electrons ($2s_2$ $2p_2$) and uranium atoms with 14 valence electrons ($6s_2$ $6p_6$ $7s_2$ $5f_3$ $6d_1$) as already was used in a previous work.[22] The Brillouin zone was integrated using 17 × 17 × 17 k-point set generated with the Monkhorst−Pack method[23] centered at the Γ point with an optimized 800 eV energy cutoff. Full bulk relaxations were performed using the conjugate gradient algorithm. Density of states (DOS) calculations were performed at the equilibrium volume with a 21 × 21 × 21 k-points grid using the tetrahedral method with Blöchl corrections for better accuracy.[24] The atomic radii used were the recommended values for the pseudopotentials used in this study: 1.588 Å for U atoms and 1.000 Å for C atoms. Al and site projected DOS also were calculated.

Results and Discussion

According to the literature, the uranium atoms in UC occupy a fcc lattice. Two structural models then were proposed for the carbon position: the NaCl ($Fm3m$) type, in which the carbon atoms occupy the octahedron vacancies, and a ZnS ($F\bar{4}3m$) type, in which the carbon atoms occupy the tetrahedral vacancies.

Figure 1 shows the experimental diffraction pattern of UC powder. It is compared with the adjusted (FullProf code) pattern of UC calculated from both $Fm3m$ (NaCl type) and $F\bar{4}3m$ (ZnS type) space groups. Both adjustments led to the same lattice parameter equal to 4.961(1) Å (conventional Rietveld reliability factors: $R_p = 65.6$, $R_{wp} = 52.1$, and $R_{exp} = 14.00$). Comparing the relative intensity of the (111) and (200) lines between the experimental diffraction patterns and both adjusted patterns (experimental: $I_{(200)}/I_{(111)} = 0.72$; NaCl type: $I_{(200)}$/

(9) Matz, W.; Schell, N.; Bernhard, G.; Prokert, F.; Reich, T.; Claubner, J.; Oehme, W.; Schlenk, R.; Dienel, S.; Funke, H.; Eichhorn, F.; Betzl, M.; Pröhl, D.; Strauch, U.; Hüttig, G.; Krug, H.; Neumann, W.; Brendler, V.; Reichel, P.; Denecke, M. A.; Nitsche, H. *J. Synchrotron Rad.* **1999**, *16*, 1076.
(10) Ravel, B.; Newville, M. *J. Synchrotron Rad.* **2005**, *12*, 537.
(11) Rehr, J. J.; Albers, R. C. *Rev. Mod. Phys.* **2000**, *72*, 621.
(12) Nilsson, H. J.; Tyliszczak, T.; Wilson, R. E.; Werme, L.; Shuh, D. K. *Anal. Bioanal. Chem.* **2005**, *383*, 41.
(13) Rodriguez Carvajal, J.; Fernandez Diaz, M. T.; Martinez, J. L. *J. Phys.: Condens. Matter* **1991**, *3*, 3215.
(14) Kresse, G.; Hafner, J. *Phys. Rev. B: Condens. Matter Mater. Phys.* **1993**, *47*, 558.
(15) Kresse, G.; Hafner, J. *Phys. Rev. B: Condens. Matter Mater. Phys.* **1994**, *49*, 14251.
(16) Kresse, G.; Furthmüller J, *Comput. Mater. Sci.* **1996**, *6*, 15.
(17) Kresse, G.; Furthmüller J, *Phys. Rev. B: Condens. Matter Mater. Phys.* **1996**, *54*, 11169.
(18) Perdew, J. P.; Wang, Y. *Phys. Rev. B: Condens. Matter Mater. Phys.* **1992**, *45*, 13244.
(19) Perdew, J. P.; Chevary, J. A.; Vosko, S. H.; Jackson, K. A.; Pederson, M. R.; Singh, D. J.; Fiolhais, C. *Phys. Rev. B: Condens. Matter Mater. Phys.* **1992**, *46*, 6671.
(20) Shöderlind, P.; Eriksson, O.; Johansson, B.; Wills, J. M. *Phys. Rev. B: Condens. Matter Mater. Phys.* **1994**, *50*, 7291.
(21) Blöchl, P. E. *Phys. Rev. B: Condens. Matter Mater. Phys.* **1994**, *50*, 17953.
(22) Perron, H.; Domain, C.; Roques, J.; Drot, R.; Simoni, E.; Catalette, H. *Inorg. Chem.* **2006**, *45*, 6568.
(23) Monkhorst, H. J.; Pack, J. D. *Phys. Rev. B: Condens. Matter Mater. Phys.* **1976**, *13*, 5188.
(24) Blöchl, P. E.; Jepsen, O.; Anderson, O. K. *Phys. Rev. B: Condens. Matter Mater. Phys.* **1994**, *49*, 16223.

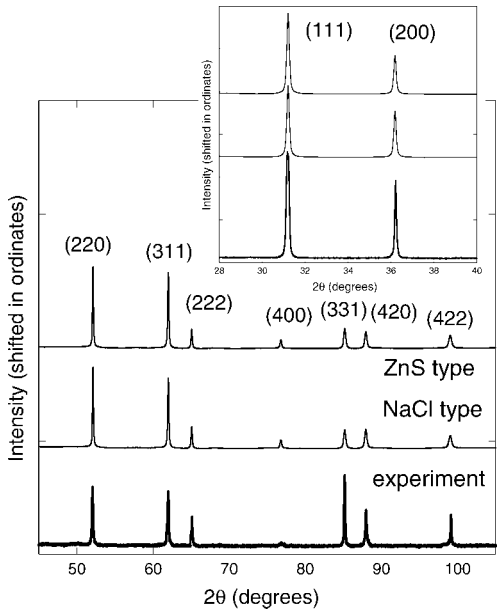

Figure 1. Experimental powder pattern of UC (bottom) as compared to calculated (FullProf, pattern matching) powder patterns based on ZnS structural type (top) and NaCl structural type (middle). The inset shows the detail of the (111) and (200) lines.

$I_{(111)} = 0.66$; and ZnS type: $I_{(200)}/I_{(111)} = 0.47$) suggests that the ZnS type can be rejected. However, a similar comparison with both (331) and (420) lines (experimental: $I_{(331)}/I_{(420)} = 1.92$; NaCl type: $I_{(331)}/I_{(420)} = 0.99$; and ZnS type: $I_{(331)}/I_{(420)} = 1.27$) suggests the opposite result. In both cases, the intensity ratios are relatively far from the calculated pattern. This may mostly be explained by the presence of preferred orientations in the sample, as already reported.[6,7] Consequently, the diffraction pattern analysis does not lead to a definite conclusion concerning the crystal structure of UC.

To distinguish between the two possible patterns, EXAFS spectra were recorded at the uranium L_{III} edge. EXAFS is mostly sensitive to first neighbors and should be able to distinguish between both types of carbon atoms (i.e., tetrahedral or octahedral sites). In a first step, the two EXAFS spectra of uranium in the NaCl and ZnS structural types were simulated (Feff82 code) with a lattice parameter of 4.96 Å. No further parameter adjustment was allowed in this simulation. Figure 2 compares the two simulated spectra of UC. The 4–7 $Å^{-1}$ region exhibits significant differences in the EXAFS oscillations of both simulated spectra: the oscillation at 4.7 $Å^{-1}$ is shifted (vertical line in Figure 2), and the intensity of the oscillation at 6.0 $Å^{-1}$ is different. A phenomenological comparison of the two simulated spectra with the experimental spectrum suggests that only the NaCl type reproduces the EXAFS oscillations, particularly in the 4–7 $Å^{-1}$ region. This result is in agreement with the conclusion of Litz and co-workers[6] based on the analysis of the diffraction pattern and the conclusion of Austin based on neutron diffraction studies.[8] Furthermore, Figure 2 provides the fitted experimental spectrum, based on the NaCl structural type. The fit is of satisfactory quality from $k = 2-15$ $Å^{-1}$. Table 1 provides the fit parameters. Note that in the fitting procedure, only one structural variable, the U−C distance, was allowed to float. The lattice parameter is

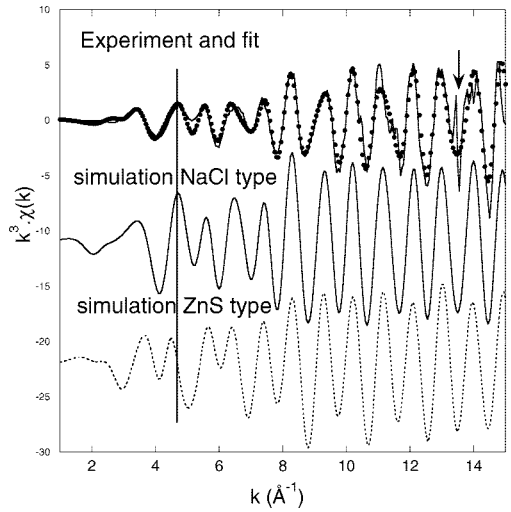

Figure 2. Experimental and calculated EXAFS spectra of UC at the uranium L_{III} edge. Top curves: experimental (solid line) and adjusted data (dots) assuming the NaCl structural type and middle and bottom curves: simulated data (no refinement) based on NaCl and ZnS structural types. The arrow on the experimental spectrum indicates a glitch.

Table 1. EXAFS Best Fit Parameters of UC at the Uranium L_{III} Edge

first neighbors	number, distance σ^2	S_0^2, e_0	$\Delta(k)$, CHI^2_r, r
U−C	*6* at 2.48(1) Å, $\sigma^2 = 0.0075$ Å^2	0.4, −2.36 eV	37×10^{-4}, 0.1
U−U	*12* at *3.51* Å, $\sigma^2 = 0.0037$ Å^2		4.7%

S_0^2 is the global amplitude factor; e_0 is the energy shift with respect to the energy threshold; $\Delta(k)$ is the measurement uncertainty in R space; CHI^2_r is the reduced CHI^2 of the fit; and r is the quality factor of the fit. Numbers in italics were fixed or linked as explained in the Experimental Procedures.

simply given by 2 times this distance and equals 4.96(2) Å, in remarkable agreement with the refinement of the diffraction pattern. Both U−C and U−U distances also are in perfect agreement with the distances obtained by neutron diffraction in the work of Austin (U−C at 2.48 Å and U−U at 3.50 Å).[8]

To better characterize the electronic behavior of the uranium atoms in the UC structure, XANES spectra at both uranium L_{III} and uranium $N_{IV,V}$ edges were recorded. XANES is a spectroscopic probe of the valence orbitals that are allowed by the selected dipolar transition (formally $2p(j = 3/2) - 6d$ for the L_{III} edge and $4d(j = 3/2, j = 5/2) - 5f$ for the $N_{IV,V}$ edges of uranium). It is well-known that the relative position of the absorption edge depends on the central atom effective charge. Figure 3a compares the L_{III} edges of UC, uranium(0) metal, and freshly prepared UO_2. The inflection point of the absorption threshold, calculated from the spectrum first derivative, is shifted from 17165.3(4) eV for U metal to 17167.3(4) eV for UC to 17170.1(4) eV for UO_2. This shift to higher energy is in agreement with a slight increase of the uranium positive charge from the U metal to UC to UO_2. On the other hand, the maximum of the absorption edge lies in the order 17175.7(4) eV for UO_2, 17177.1(4) eV for U metal, and 17177.8(4) eV for UC. This discrepancy is attributed to the sensitivity of the edge shape (and, in particular, edge maximum) to the central atom local structure. Also, the strong self-absorption for the U metal

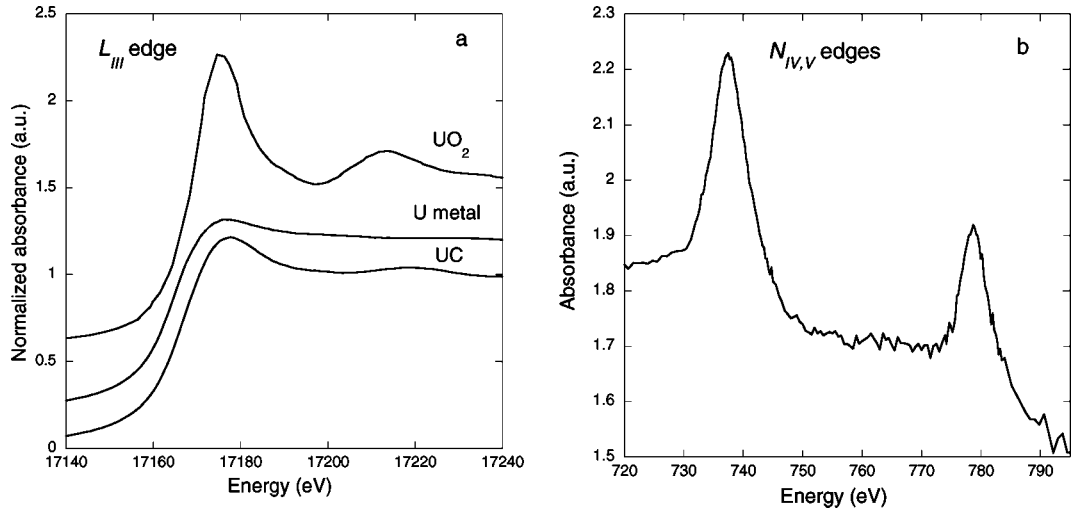

Figure 3. (a) XANES L_{III} edges of uranium in metallic uranium, UC, and UO_2. Spectra were not corrected for self-absorption. (b) XANES $N_{IV,V}$ edges of uranium in UC.

and UC samples might induce a distortion of the edge maximum. Because L edges are very sensitive to scattering features, the position of the edge ramp also is sensitive to the central atom polyhedron. On the contrary, the $N_{IV,V}$ edges in Figure 3b correspond to more atomic-like transitions that directly probe the 5f states. The maximum of the N_V edge at 737.5 eV lies in between the values reported by Nilsson and co-workers in the literature:[12] 736.4 eV for U metal and 738.5 eV for UO_2. This position of the UC edge confirms the observation at the L_{III} edge, suggesting that the electronic charge borne by the uranium atom is intermediate between that in U metal and that in uranium dioxide.

To corroborate these first results, the UC electronic structure was calculated and compared to the α-U structure. First, a full structural relaxation was performed to obtain crystallographic parameters of both UC and α-U structures. Only the NaCl type structure (*Fm3m* space group) was considered, taking into account the obtained experimental results. The unit cell is displayed in Figure 4a. UC calculated geometrical parameters were in good agreement with the EXAFS results (d(U−C) = 2.47 Å and d(U−U) = 3.49 Å). Moreover, starting from the α-U experimental structure (face-centered orthorhombic unit cell displayed in Figure 4b), the full relaxation led to calculated parameters (a = 2.827 Å, b = 5.845 Å, c = 4.923 Å and y = 0.100), in good agreement with experimental[25] values as well as previous DFT calculations[26,27] presented in Table 2. Calculations of the partial density of states of α-U5f are displayed in Figure 5a. States below the Fermi level were occupied, and states above the Fermi level were unoccupied (the Fermi level being 0 eV). This partial DOS-5f is very similar to the one calculated by Tobin et al.[28] Two peaks can be identified: the first peak around 0.6 eV corresponds to the α-U5f5/2 contribution, and

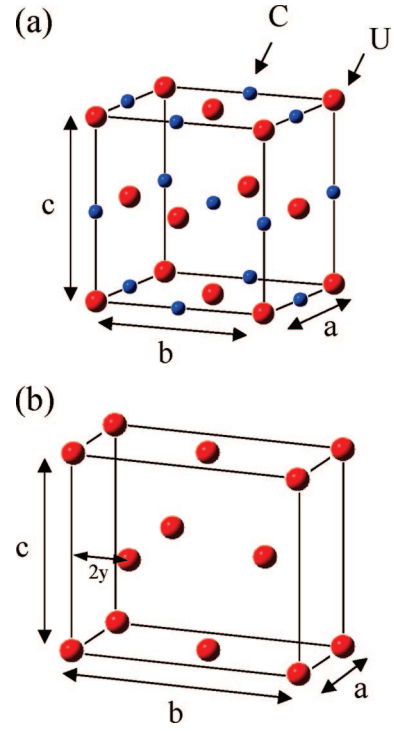

Figure 4. (a) UC crystal structure (NaCl type (*Fm3m*)) and (b) α-U crystal structure (face-centered orthorhombic unit cell (*Cmcm*)).

Table 2. Structural Study of the α-U Phase

	V_0 (Å^3)	a (Å)	b (Å)	c (Å)	b/a	c/a	y (Å)
this work	20.33	2.827	5.845	4.923	2.067	1.741	0.100
DFT[19]							
GGA	19.49						
LDA	18.33						
DFT-LDA[26]	18.90	2.805	5.438	4.956	1.939	1.767	0.107
DFT-GGA[27]	20.67	2.845	5.818	4.996	2.044	1.756	0.102
experimental[25] (measured at 40 K)	20.52	2.836	5.866	4.935	2.068	1.740	0.102

V_0 is the equilibrium volume, a is the cell parameter, and b/a, c/a, and y are the internal parameters.

a second peak at around 2.5 eV corresponds to the α-U5f7/2 part. The partial DOS of C2p and U5f are displayed in Figure 5b. The main part of the C2p states is located below the Fermi level between –3.5 and –0.5 eV. The main part of the

(25) Barett, C. S.; Mueller, M. H.; Hittermann, R. L. *Phys. Rev.* **1963**, *129*, 625.
(26) Crocombette, J. P.; Jollet, F.; Nga, L. T.; Petit, T. *Phys. Rev.* **2001**, *64*, 104107.
(27) Shöderlind, P. *Phys. Rev. B: Condens. Matter Mater. Phys.* **2002**, *66*, 85113.
(28) Tobin, J. G.; Moore, K. T.; Chung, B. W.; Wall, M. A.; Schwartz, A. J.; Laan, G. v. d.; Kutepov, A. L. *Phys. Rev. B: Condens. Matter Mater. Phys.* **2005**, *72*, 85109.

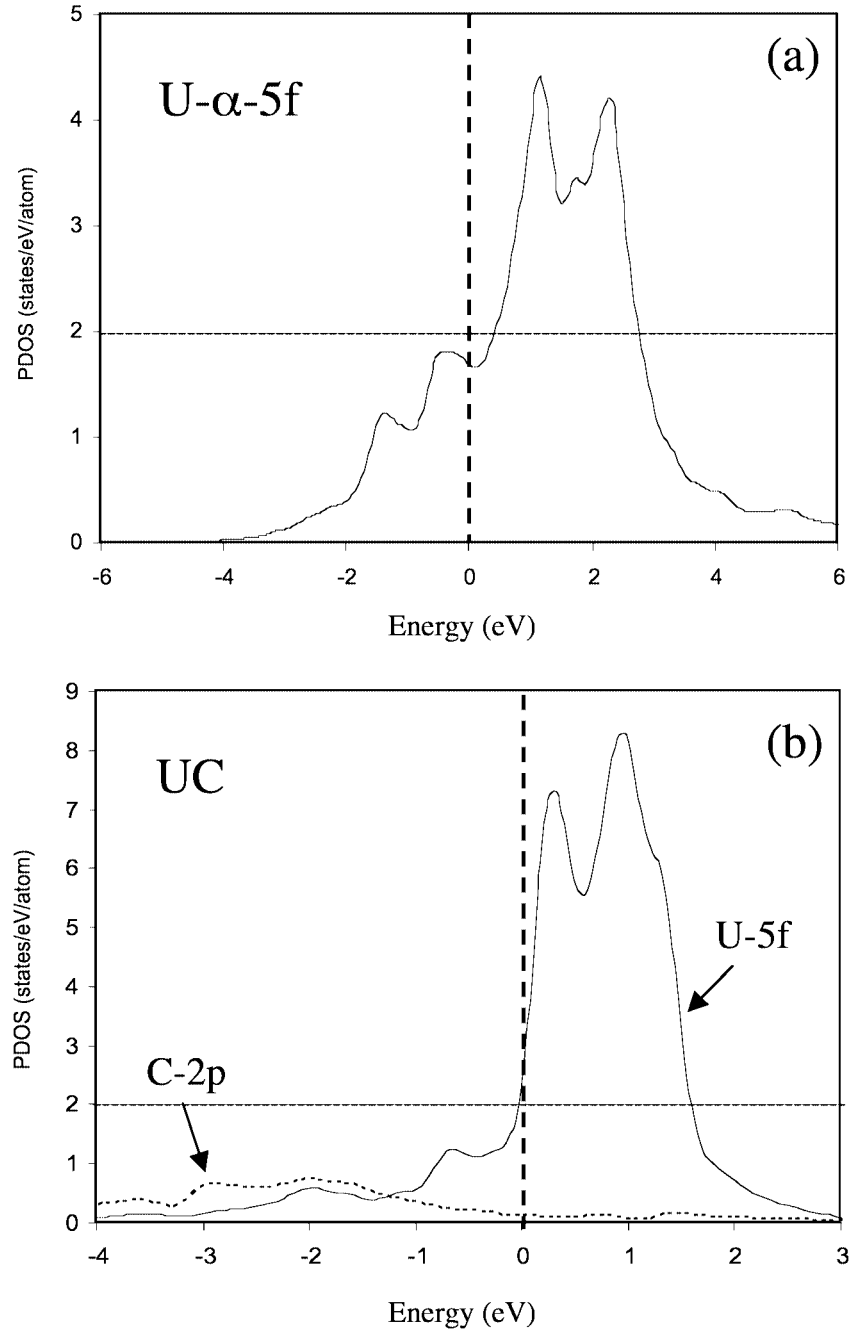

Figure 5. (a) α-U5f partial density of states and (b) U-5f and C-2p partial density of states of UC.

U5f states is situated in the energy range of –3 eV/2.5 eV as was already observed for other uranium compounds.[29] It can be seen, in Figure 5b, that hybridization between these two groups of states leads to a decrease of the U5f DOS below the Fermi level relative to the α-U5f DOS (Figure 5a). This behavior shows an electron transfer from the U-5f states toward the C2p states. Even if it is difficult with this methodology (plane waves) to accurately determine the electrons' location, we compared the U5f occupation numbers of the α-U and UC systems to obtain a qualitative estimation of the electron transfer between U5f and C2p. A decrease of the occupation numbers (of around 0.6 electron) is observed from the U metal to the UC system, which is in agreement with the shift, to a higher energy, observed in the XANES spectra.

Conclusion. Former literature data on the UC phase are subject to ambiguities. In the present work, a structural and electronic reinvestigation of the UC phase was carried out with a combination of X-ray techniques and quantum chemical calculations. The X-ray powder pattern of UC obtained in this work was not conclusive to discriminate between NaCl and ZnS types of phases. To do so, complementary EXAFS simulations and EXAFS data fitting unambiguously led to the attribution of the UC crystal phase to the NaCl type, while the ZnS type could be rejected. To further investigate the electronic behavior

(29) Divis, M.; Sandratskii, L. M.; Richter, M.; Mohn, P.; Novak, P. *J. Alloys Compd.* **2002**, *337*, 48.

of uranium in the UC phase, uranium XANES images at both L_{III} and $N_{IV,V}$ edges were recorded. Both edges reflect an increase of the uranium charge because of a slight high-energy shift of the edge as one goes from the U metal to UO_2, UC having an intermediate behavior. DFT calculations on both UC and α-U metal were performed to complement the spectroscopic data. In a first step, the structural parameters of both phases were calculated with a very satisfactory agreement with the experimental (XRD and EXAFS) data. In a second step, an electron transfer from the U-5f states toward the C-2p states was observed in comparison with the α-U metal. This is in agreement with a decrease of the occupation numbers of around 0.6 electron from the U metal to UC systems and corroborates the high-energy shift of the uranium XANES spectra from the U metal to UC.

Acknowledgment. We thank CEA/DEN/DDIN/TRAC for support. XAS measurements were carried out at the former LURE facility (Orsay, France), D44 beamline and ESRF (Grenoble, France), BM20 (a CRG beamline of FZD, Rossendorf, Germany), and the Advanced Light Source (Berkeley, CA) supported by the Office of Science, Office of Basic Energy Sciences of the U.S. Department of Energy under Contract DE-AC02-05CH11231 at LBNL. The authors thank A. Scheinost, H. Funke, and C. Hennig from the Forshungzemtrum Dresden Rossendorf, ROBL for their help.

CM8001783